

Proton Therapy Treatment Verification via PET Imaging

Joanne Beebe-Wang

P. Vaska, F. A. Dilmanian, S. G. Peggs and D. J. Schlyer
Brookhaven National Laboratory, Upton, NY, USA

Outline

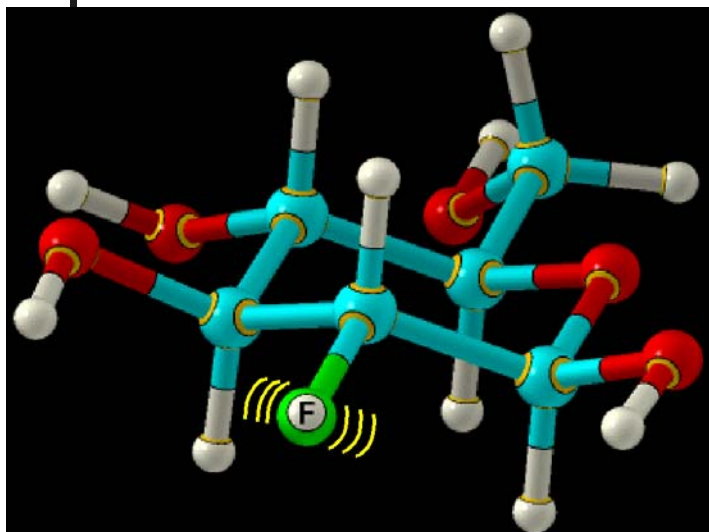
1. What is PET and how does PET work?
2. Proton Therapy and induced activity
3. Nuclear reactions producing position emitting isotopes
4. Nuclear reaction cross section data
5. Monte Carlo Simulation: SRNA-BNL
6. Isotope productions in soft tissue
7. PET image simulation
8. Determination of proton dose depth
9. Experiment with $^{12}\text{C}^{6+}$ beam of NSRL
10. Conclusion and Discussion

What is PET?

PET is a camera that takes pictures of biochemical processes in your body by using a radiotracer that sends out a signal that can be detected outside the body



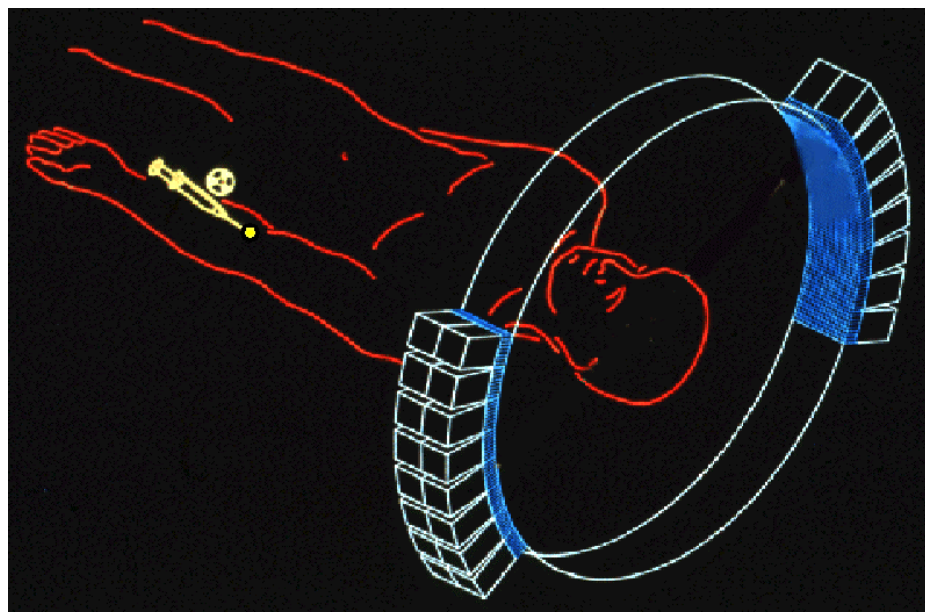
How Does PET Work?



Compounds like simple sugars (glucose for example) are labeled with these positron emitting tracers

Isotope	half-life
carbon-11	20.4 min
fluorine-18	110 min
nitrogen-13	10 min
oxygen-15	2 min

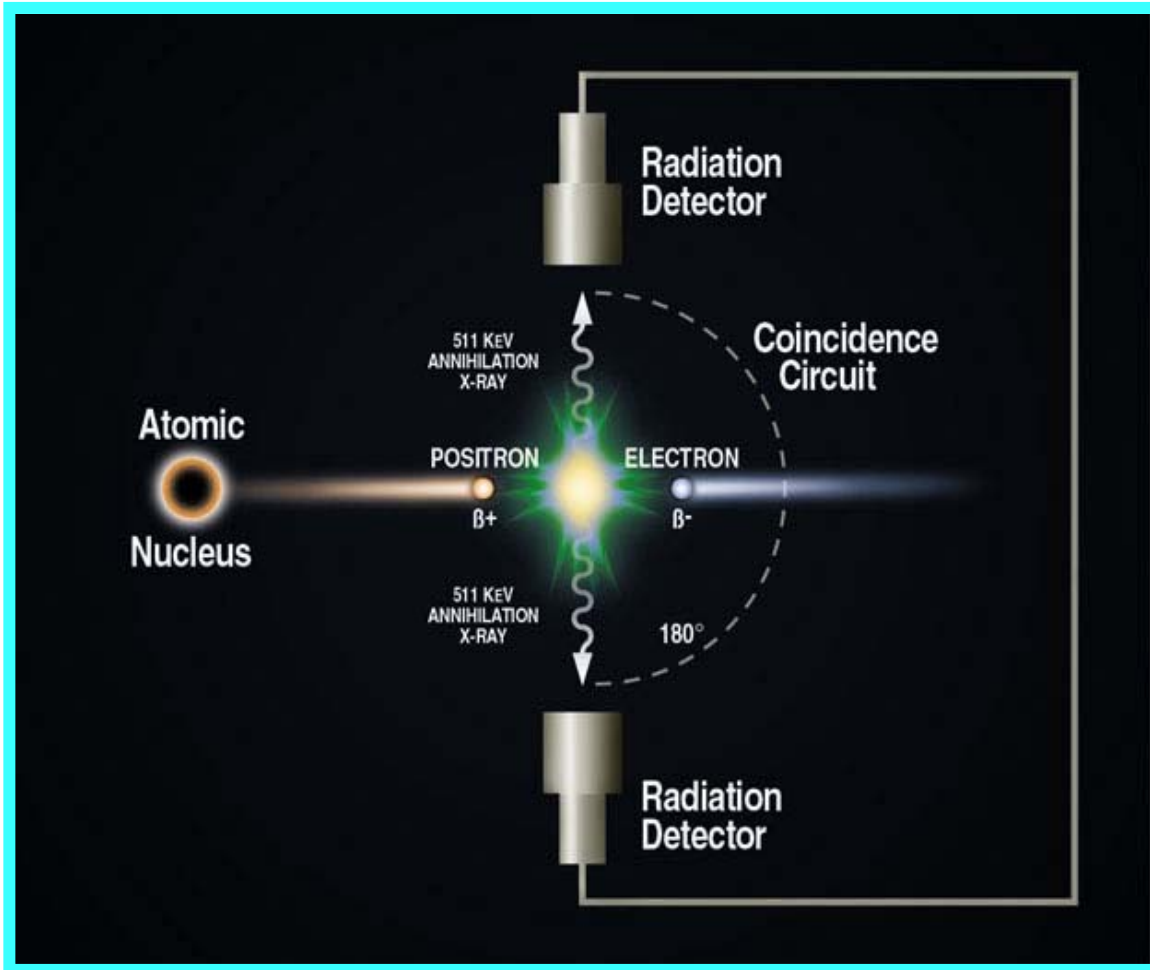
A scanner records the signals from these tracers as they travel through the body and accumulate in different organs



Human PET Scanner

Radioisotopes Decay and Gamma Ray Detection

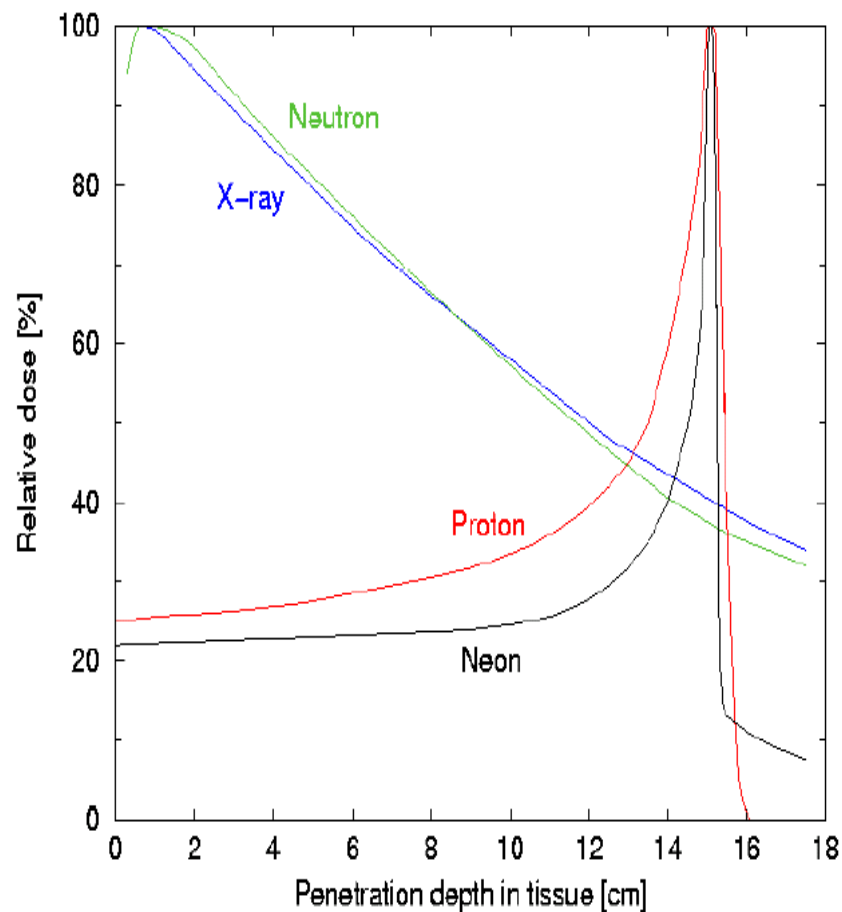
The radioisotopes react with the molecules in the body, and decay to stability by emitting positrons. When a positron encounters an electron in the surrounding tissue, the two particles annihilate turning the mass of the two particles into two 511 keV γ -rays with opposed momenta. These γ -rays escape from the human body and can be recorded by external detectors.



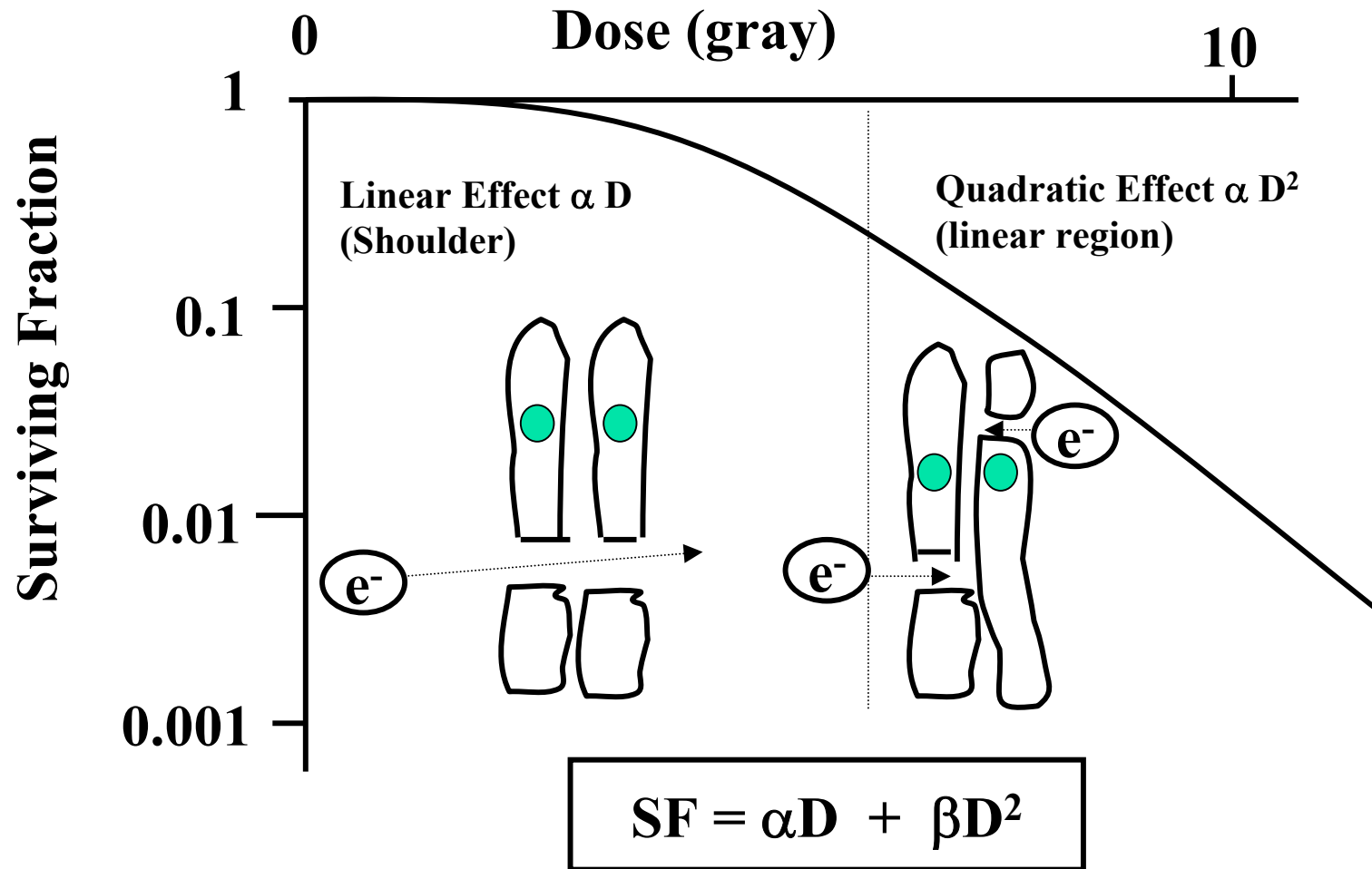
Proton therapy & PET imaging

1. Proton therapy is increasingly used because the dose conforms more tightly to the tumor than x-ray therapy.
2. Protons produces positron-emitting isotopes along the beam path through nuclear reactions.
3. The PET image is essentially the negative image of the target volume because the signal along the beam path diminish at the Bragg peak.
4. Verification of the therapy can be achieved by comparing the PET images with the predicted target dose distribution used in planning.

Relative dose distributions



Survival of Irradiated Cells



Unclear Reactions Producing Positron Emitting Isotopes

The expected number of nuclear reactions is governed by three factors:

- Nuclear reaction cross section
- The number of incoming particles
- The number of target particles.

The nuclear reaction cross section σ is defined to be the probability P of the interaction for one target nucleus, when subjected to the particle flux Φ :

$$\sigma = P / \Phi$$

Express the depth z as a function of energy E by numerically integrating the inverse of the stopping Power:

$$z(E) = \int_{E_0}^E \left(\rho_T \left| \frac{dE}{d\lambda} \right|_T \right)^{-1} dE$$

	Soft Tissue	Lucite	Water
Density	1	1.19	1
Oxygen	76.18%	31.96%	11.19%
Nitrogen	2.60%		
Carbon	11.10%	59.99%	
Hydrogen	10.12%	8.05%	88.81%

The number N_{ip} of positron emitter type i produced by nuclear reaction process p is governed by the rate of production and decay:

$$\frac{dN_{ip}(\vec{r}, t)}{dt} = \sigma_{ip}(E(\vec{r})) \Phi(\vec{r}, t) n_i(\vec{r}) A dz - \lambda_i N_{ip}(\vec{r}, t)$$

Unclear Reactions Producing Positron Emitting Isotopes

	Reaction	Threshold Energy (MeV)	Q-Value (MeV)	Cross Section (NNDC Exp.) E. Range (MeV)	Cross-Section (Mukhopadhyay) E. Range (MeV)	Half-life Time (min)	Positron Decay %	Positron Max. E. (MeV)	Daughter Nuclide
1	O16 (p, n+p) O15	16.7917(6)	_15.6637(5)	15-156	0-160	2.037	99.9	1.72	N15 stable
2	N15 (p, n) O15	3.7910(6)	_3.5363(5)	4.0-13					
3	O17 (p, 2n+p) O15	21.2334(8)	_19.8070(7)	N/A					
4	O18 (p, 3n+p) O15	29.8571(11)	_27.8514(11)	N/A					
5	O16 (gamma, n) O15	15.6637(5)	_15.6637(5)	15.1-24.9					
6	O16 (p, alpha) N13	5.6567(3)	_5.2184(3)	6.7-28.7		9.965	100	1.19	C13 stable
7	O16 (p, 2n+2p) N13	36.3293(3)	_33.5141(3)	14-150	0-160				
8	N14 (p, n+p) N13	11.4398(3)	_10.5534(3)	12.6-156	0-160				
9	C13 (p, n) N13	3.2550(3)	_3.0028(3)	0-33					
10	N15 (p, 2n+p) N13	23.1831(3)	_21.3867(3)	N/A					
11	O17 (p, 3n+2p) N13	40.8206(6)	_37.6574(6)	N/A					
12	O18 (p, 4n+2p) N13	49.5407(10)	_45.7108(10)	N/A					
13	N14 (gamma, n) N13	10.5534(3)	_10.5534(3)	10.5-15.5					
14	C12 (p, n+p) C11	20.6080(11)	_18.7219(10)	50-383, 0.4-28G	0-160	20.39	99.8	0.96	B11 stable
15	N14 (p, alpha) C11	3.2175(11)	_2.9231(10)	3.8-22.6					
16	N14 (p, 2n+2p) C11	34.3639(11)	_31.2187(10)	13 only	0-160				
17	O16 (p, 3p3n) C11	59.6378(11)	_54.1794(10)	222-362	0-160				
18	C13 (p, 2n+p) C11	26.0526(11)	_23.6682(10)	18.2-30.6					
19	N15 (p, alpha+n) C11	15.1423(11)	_13.7564(10)	17.7-29.8					
20	N15 (p, 3n+2p) C11	46.2886(11)	_42.0520(10)	N/A					
21	C12 (gamma, n) C11	18.7219(10)	_18.7219(10)	18.0-51.8					
22	O18 (p, n) F18	2.5824(7)	_2.4378(7)	2.3-14.7		109.7	96.9	0.635	O18 stable

Uncommon Reactions Producing Positron Emitting Isotopes

Uncommon Nuclear Reactions

Nuclear Reactions	Threshold Energy (MeV)	Half-life Time (min)	Positron Max. Energy (MeV)
$^{12}\text{C}(p,p2n)^{10}\text{C}$	34.5	0.32	1.87
$^{12}\text{C}(p,\gamma)^{13}\text{N}$	0	9.97	1.19
$^{13}\text{C}(p,p2n)^{11}\text{C}$	25.5	20.3	0.96
$^{13}\text{C}(p,n)^{13}\text{N}$	3.2	9.97	1.19
$^{14}\text{N}(p,n\alpha)^{10}\text{C}$	17.2	0.32	1.87
$^{14}\text{N}(p,\gamma)^{15}\text{O}$	0	2.04	1.72
$^{14}\text{N}(p,n)^{14}\text{O}$	6.6	1.18	1.81
$^{15}\text{N}(p,n\alpha)^{11}\text{C}$	14.7	20.3	0.96
$^{15}\text{N}(p,nd)^{13}\text{N}$	20.4	9.97	1.19
$^{15}\text{N}(p,t)^{13}\text{N}$	13.8	9.97	1.19
$^{15}\text{N}(p,n)^{15}\text{O}$	3.8	2.04	1.72
$^{16}\text{O}(p,\gamma)^{17}\text{F}$	0	1.07	1.74
$^{16}\text{O}(p,3p4n)^{10}\text{C}$	39.1	0.32	1.87
$^{16}\text{O}(p,p2n)^{14}\text{O}$	30.7	1.18	1.81
$^{18}\text{O}(p,n)^{18}\text{F}$	2.6	109.8	0.64

These nuclear reactions are not included in the study because:

1. ^{13}C , ^{15}N and ^{18}O are rarely found in the human body.
2. The cross sections of the radioactive capture reactions, (p,γ) , are typically three orders of magnitude smaller than the six main reactions.
3. Very small quantities of production of ^{10}C and ^{14}O isotopes.

Relevant Positron-Emitter Production Reactions

Nuclear Reactions	Threshold Energy (MeV)	Half-life Time (min)	Positron Max. Energy (MeV)
$^{12}\text{C}(\text{p},\text{pn})^{11}\text{C}$	20.61	20.39	0.96
$^{16}\text{O}(\text{p}, \text{pn})^{15}\text{O}$	16.79	2.04	1.72
$^{16}\text{O}(\text{p},2\text{p}2\text{n})^{13}\text{N}^{\text{a)}}$	5.66 ^{c)}	9.97	1.19
$^{16}\text{O}(\text{p},3\text{p}3\text{n})^{11}\text{C}^{\text{b)}}$	27.50 ^{c)}	20.39	0.96
$^{14}\text{N}(\text{p},\text{pn})^{13}\text{N}$	11.44	9.97	1.19
$^{14}\text{N}(\text{p}, 2\text{p}2\text{n})^{11}\text{C}^{\text{a)}}$	3.22 ^{c)}	20.39	0.96
a): (p,2p2n) is inclusive of (p, α)			
b): (p, 3p3n) is inclusive of (p, α pn)			
c): The listed thresholds refer to (p, α) and (p, α pn)			

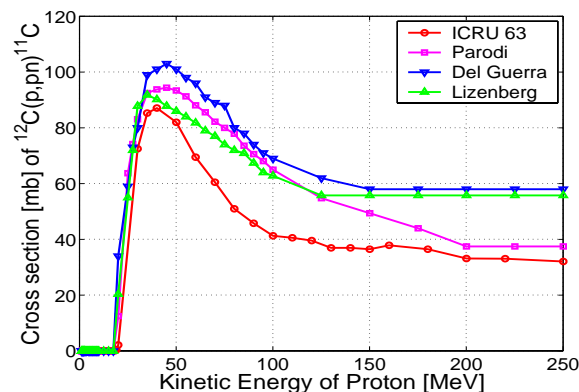
Cross Section Data Resources

Four sets of nuclear reaction cross section data were used:

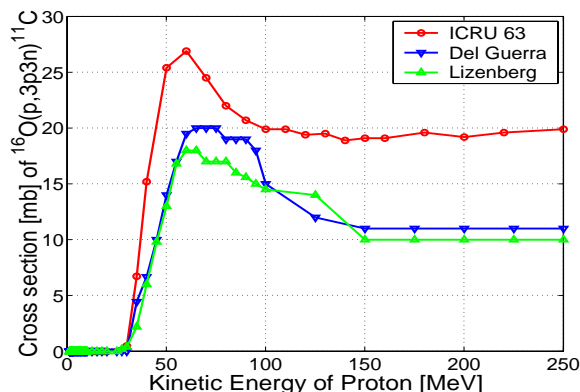
- 1). Data extracted from the emission spectra of recoils in the ENDF electronic file provided by the ICRU (International Commission on Radiation Units and Measurements) Report 63 [2000] used by J. Beebe-Wang et al. [Proceedings of IEEE MIC 2003]; [Proceedings of EPAC 2002, p.2721, 2002];
- 2). Data from "Experimental Nuclear Reaction Data File (EXFOR)" maintained by National Nuclear Data Center at BNL used by K. Parodi et al. [Phys. Med. Biol. 47 p.21-26, 2002];
- 3). Data from TERA 95/19 TRA15 [1995] used by A. Del Guerra et al. in reference [TERA 93/10 TRA 9, 1993];
- 4). Data from 8 different resources during 1962-1996 collected by D. Litzenberg in his Ph.D. dissertation [Univ. of Michigan, 1997].

Nuclear Reaction Cross Section Data

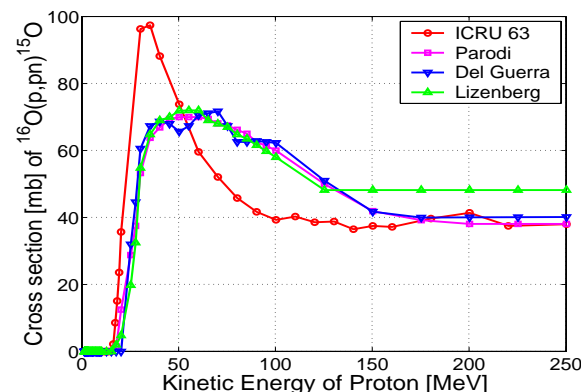
$^{12}\text{C}(p, pn)^{11}\text{C}$



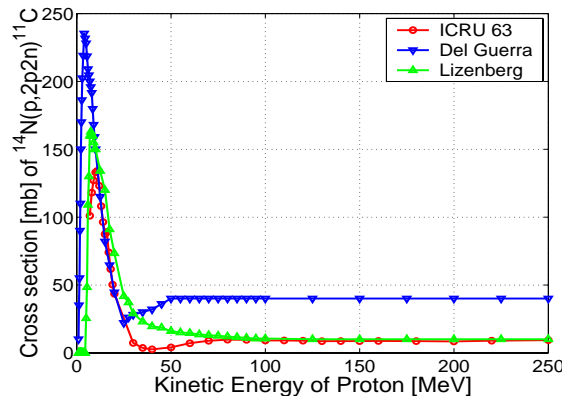
$^{16}\text{O}(p, 3p3n)^{11}\text{C}$



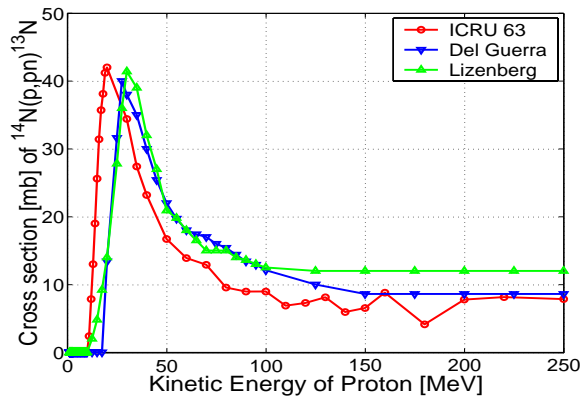
$^{16}\text{O}(p, pn)^{15}\text{O}$



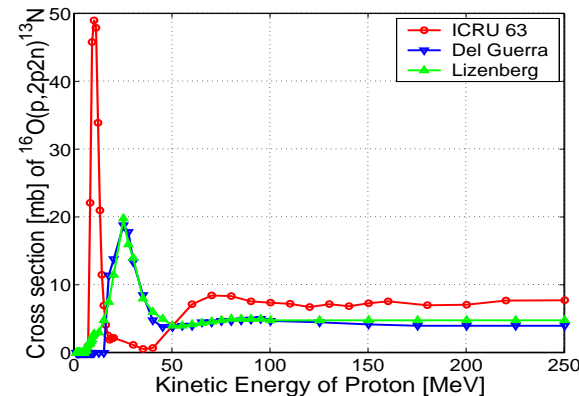
$^{14}\text{N}(p, 2p2n)^{11}\text{C}$



$^{14}\text{N}(p, pn)^{13}\text{N}$



$^{14}\text{N}(p, pn)^{13}\text{N}$



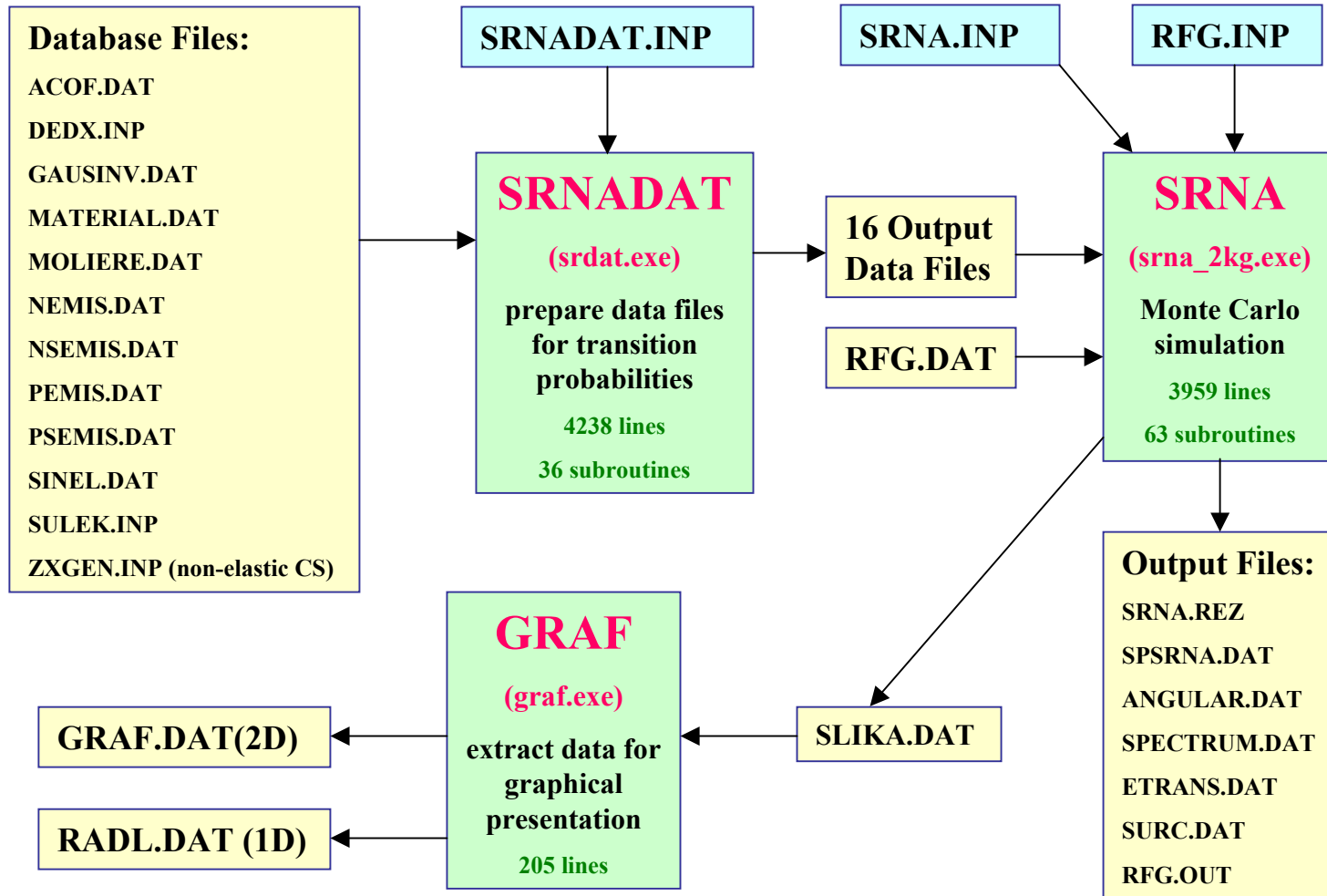
Monte Carlo Simulation Codes for Proton Transport

MC Code	Year	Projectile	Medium	Dimension	Min E	Max E	Principal Application
MOCA13	1981	p, alpha	water			4MeV	
OREC	1983	p, alpha	water			4MeV	
TRIM	1985	ions	solids			1GeV	
PARTRAC	1992		water				
TRION	1993	p, alpha	water			4MeV	
PTRAN	1993	p	water	1D/3D	50MeV	250MeV	proton therapy
MOCA13	1994	p, alpha	water			20MeV	
PITS	1994	ions	all		0.3MeV		
TRK	1994	ions	several			1GeV	
STRBSOL	1996	ions	water				
PETRA	1997	p,e,alpha	water	cylindrical	50MeV	250MeV	proton therapy
GEANT-3	1974-now	almost all	user defined	3D	0	20TeV	high energy physics
FLUKA	1982-now	almost all	user defined	3D	0	20TeV	high energy physics
GEANT-4	1994-now	almost all	user defined	3D	0	20TeV	high energy physics
SRNA-2KG	1998-now	p	user defined	3D	100keV	250MeV	proton therapy
TRAX	2000-now	ions, p, e	user defined	3D	0	few MeV	radiation

SRNA-2KG Package

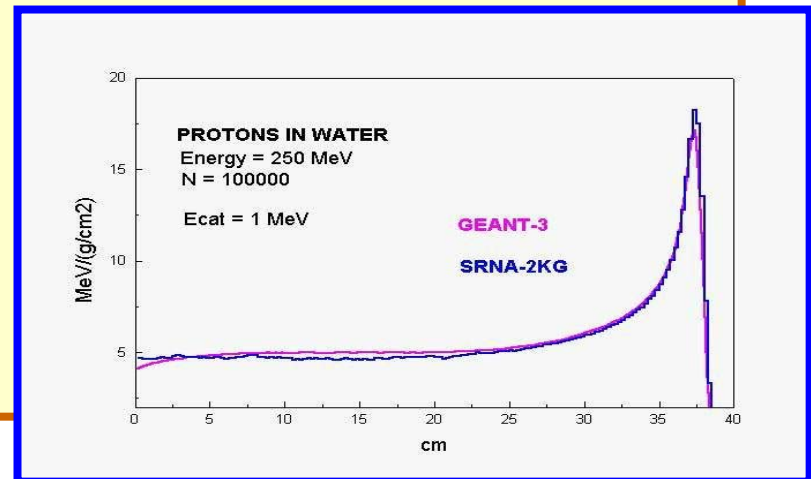
Original Author	Radovan D. Ilic, Ph.D., Institute for Nuclear Sciences, Yugoslavia
General Purpose	Numerical experiments for radiotherapy and dosimetry
Method	Monte Carlo
Transport Particle	proton only
Energy Range	100keV to 250MeV
Material Database	total type: 279. Elements: Z=1-99. Compounds and mixtures: 181
Material Geometry	10 shapes of 3D -zones described by 1st and 2nd order surfaces
	a) Average energy loss (ICRU report 49; Ziegler 1985; TRIM96)
Energy Loss Model	b) Energy loss fluctuation (Vavilov 1957)
	c) Energy loss distribution correction (Schulek 1966)
Angular Dist. Model	Integration of Moliere desity function (Moliere 1948; Bethe 1953)
Nuclear interaction	total cross sections (ICRU 63; Young and Chadwick 1997)
	a) protons (transported as the protons from source)
Secondary particles	b) deuterons, tritons, alphas (absorbed at the place of creation)
	c) neutrons, photons (not treated, the distributions are recorded)
spectra of recoils	Not included (included in SRNA-BNL)
Program Language	FORTRAN 77
Computer platform	PC Windows (changed to Linux for SRNA-BNL)
Compiler	MS FORTRAN PowerStation

SRNA-2KG Package



Simulation Code: SRNA-BNL

- Monte Carlo code SRNA-2KG originally developed by R. D. Ilic [Inst. of Nucl. Science Beograd, Yugoslavia, 2002] for proton transport, radiotherapy, and dosimetry.
- Modified at BNL to include the production of positron emitter nuclei.
- Proton energy range 0.1-250 MeV with pre-specified spectra are transported in a 3D geometry through material zones confined by planes and second order surfaces.
- Can treat proton transport in 279 different kinds of materials including elements of $Z=1-98$ and 181 compounds and mixtures.
- Use multiple scattering theory and on a model for compound nucleus decay after proton absorption in non-elastic nuclear interactions.
- For each energy range, an average energy loss is calculated with a fluctuation from Vavilov's distribution and with Schulek's correction. The deflection angle of protons is sampled from Moliere's distribution.
- Benchmarked with GEANT-3 and PETRA.
A very good agreement was reached.



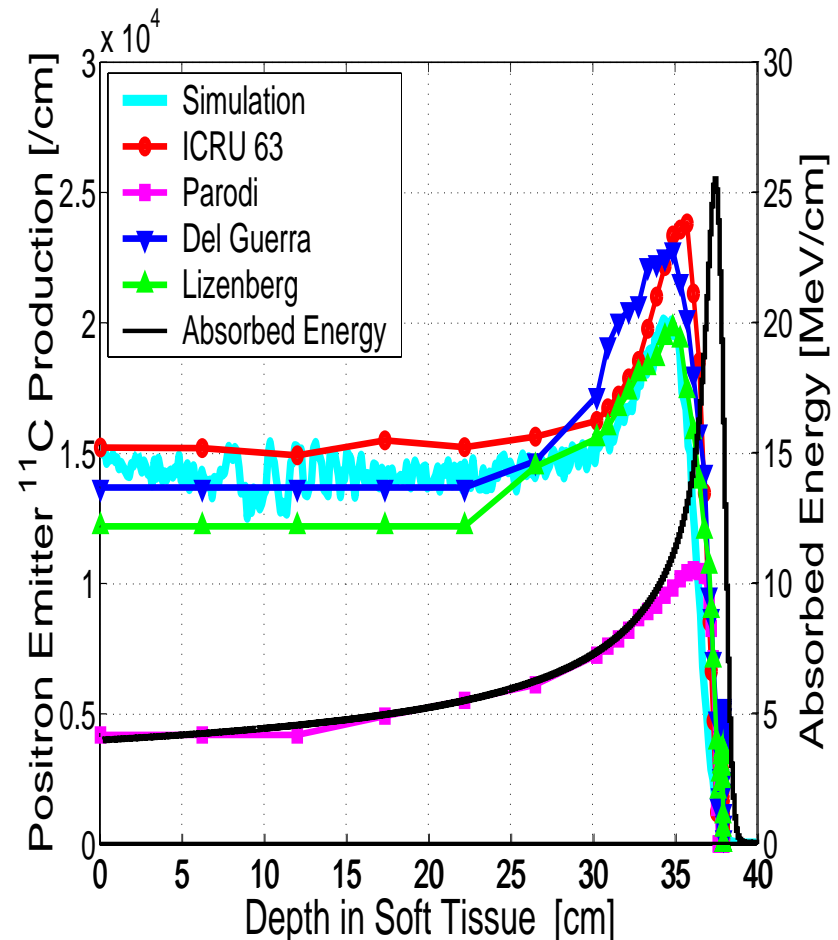
^{11}C Isotope Production in Soft Tissue

Simulation:

Cross section data: **ICRU63**
Simulation code: **SRNA-BNL**
Total sets simulated: **45**
Number of Protons: **2×10^7**
Max Kinetic Energy: **250 MeV**
Min Kinetic energy: **0.1 MeV**
Proton Beam diameter: **2 mm**
Beam divergence angle: **0**
Dose at Bragg Peak: **2 Gray**

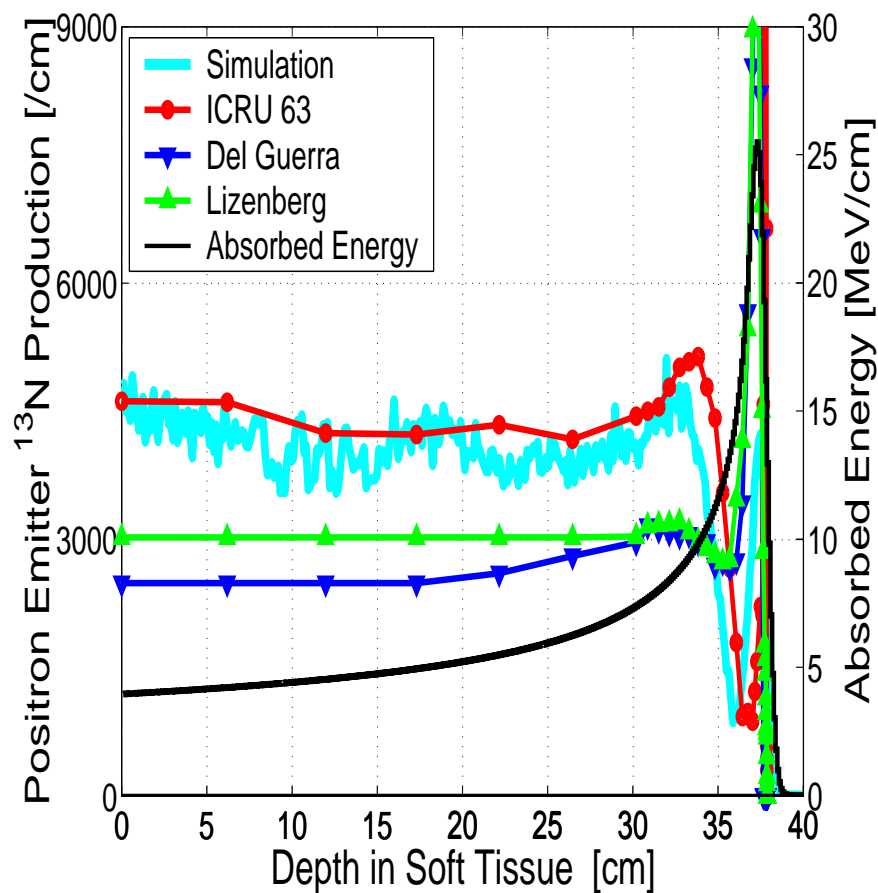
ICRU 4-component tissue:
Density: **1.0 g/cm^3**
 Z/A : **0.55**
Hydrogen: **10.11%**
Carbon: **11.11%**
Nitrogen: **2.60%**
Oxygen: **76.18%**

^{11}C Isotope (half-life time 20.39 min.)

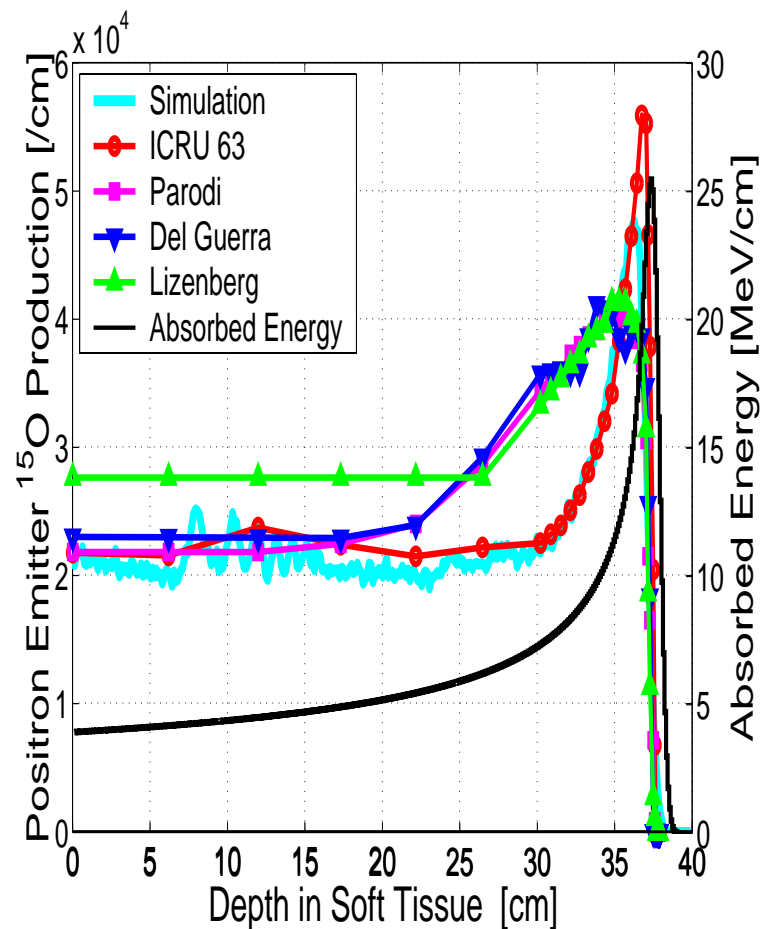


^{13}N and ^{15}O Isotopes Production in Soft Tissue

^{13}N Isotope (half-life time 9.97 min.)



^{15}O Isotope (half-life time 2.04 min.)



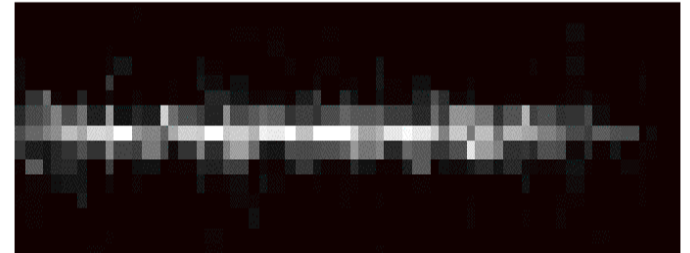
PET Image Reconstruction

Input positron emitter (^{11}C , ^{13}N , ^{15}O) distribution used in the simulation:

1. Magnitude corresponds to delivery of typical 2 Gray therapy fraction
2. Dose spread over 5 cm in depth using 5 beam energies
3. Maximum beam energy 250 MeV

SimSET Monte Carlo tomograph simulation:

1. Modified to accommodate a block detector layout and standard 3D-sinograms binning
2. Clinical whole-body CTI HR+ PET scanner with standard acquisition parameters
3. Proton beam path aligned with scanner axis
4. Attenuation of a typical human head
5. Many simulations were carried out to analyze noise
6. Standard Filtered back-projection image reconstruction

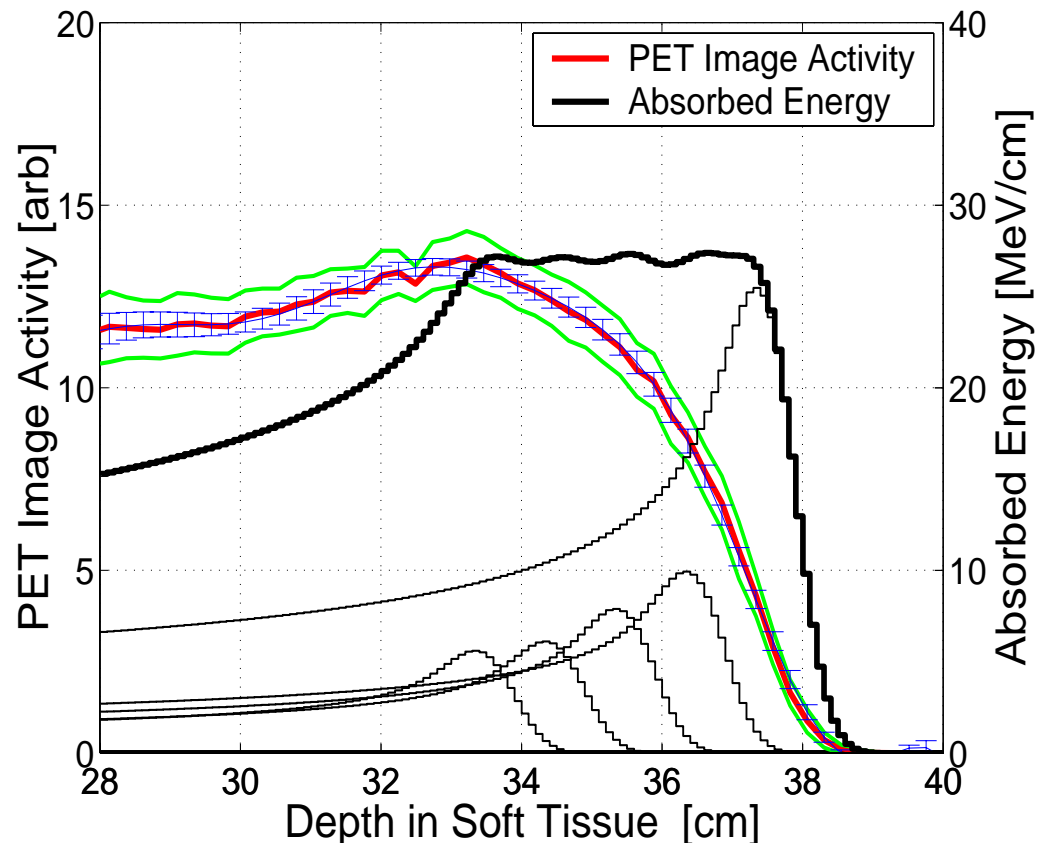


A 1.7 mm thick slice through the activity distribution of the 3-dimensional PET image. The beam entered from left. Horizontal (axial) dimension is 15.5 cm (full scanner FOV) and pixel size is 2.4 mm horizontal by 1.7 mm vertical.

Despite only about 14000 coincidence counts in the entire image, the narrow transaxial distribution and lack of background activity gives sufficient contrast to provide a reasonable definition of the distribution.

Treatment Verification via Induced Activity Determined from PET Image

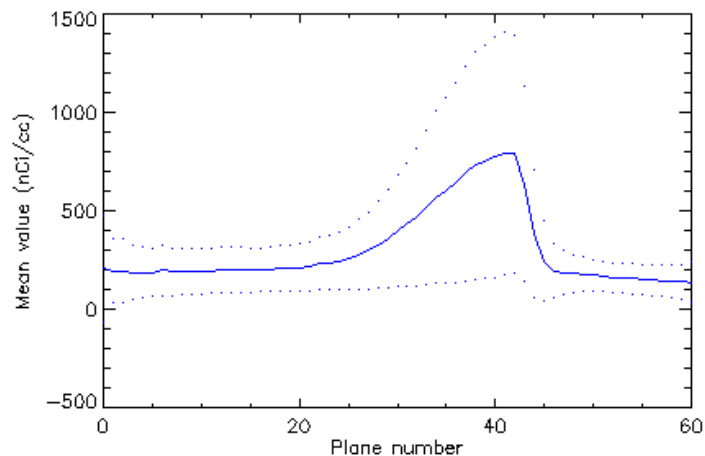
- The “spread-out Bragg peak” is created by five proton beam pulses.
- The expected PET image activity signal and its standard deviation are determined with the data extracted from 100 sets of images.
- A simply algorithm of polynomial curve fit was developed to analyze each set of noisy PET data.
- With the help of this simple software, the average value of processed data coincident with the expected PET image activity with much smaller standard deviation (error bars) compared to the one of unprocessed data.
- Depth at half maximum of PET image activity distribution is then determined to be 6.3 mm from the end of the “spread-out Bragg peak” in the soft tissue with 1 mm accuracy.



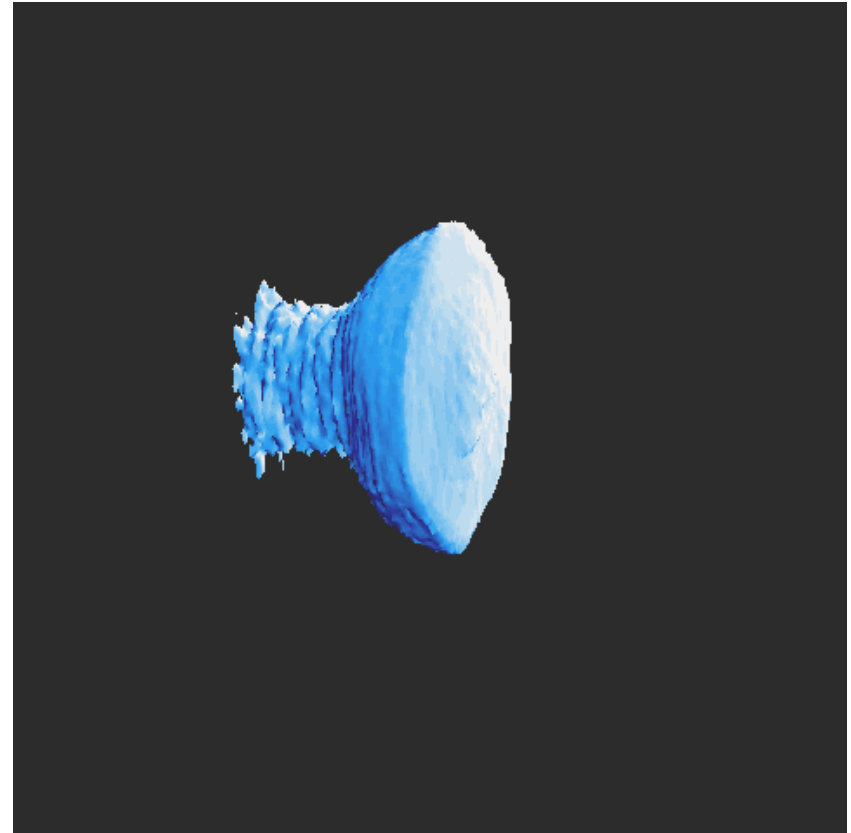
Depth distribution of induced activity as determined from PET image compared to the absorbed energy.

Experiment with $^{12}\text{C}^{6+}$ Beam on NSRL

- 06/11/2003 during the commissioning of NASA Space Radiation Laboratory (NSRL)
- $^{12}\text{C}^{6+}$ 300 MeV/nucleon $^{12}\text{C}^{6+}$ beam on Lucite
- 8×10^8 ions/pulse, 5sec/pulse, totally 10min
- Total of about 50 microCi at injection time
- microPET recorded activities for 6 hours
- Mostly from ^{11}C decay (half-time 20min)



Bragg curve



Surface-rendered 3D PET image of induced activity.

Conclusion and Discussion

- For a typical 2 Gray proton therapy session, a subsequently acquired PET image can have sufficient signal-to-noise ratio to determine the depth of the Bragg peak to ~1 mm accuracy.
- The differences in positron emitter production distributions due to the different resources of nuclear reaction cross section data are easily observed. The high yield of ^{13}N and ^{15}O in the low energy range calculated with data ICRU 63 report is credited to the cross section data which only became available during the year 2000.
- A reliable simulation or calculation depends upon accurate cross section data. There is an on going need to develop a library of accurate cross section data for proton and neutron-induced reactions on the elements in human tissue.
- A robust algorithm for fitting the PET data in the presence of noise requires more investigation for future clinical application.